Ocean Sci. J. (2012) 47(3):313-321
http://dx.doi.org/10.1007/s12601-012-0030-6

Article

Available online at www.springerlink.com

SpringerLink

Ocean Science Journal

Estimating Photosynthetically Available Radiation at the Ocean Surface from GOCI Data

Robert Frouin* and John McPherson

Scripps Institution of Oceanography, University of California San Diego, La Jolla, CA 92037, USA

Received 5 April 2012; Revised 2 July 2012; Accepted 20 August 2012

Abstract – A technique is presented to estimate photosynthetically available radiation (PAR) at the ocean surface from Geostationary Ocean Color Imager (GOCI) data. The sensor is adapted to the problem, since it measures at visible wavelengths and does not saturate over clouds, and the hourly data provides adequate temporal sampling to describe diurnal variability of clouds. Instantaneous surface PAR is computed as the difference between the solar irradiance incident at the top of the atmosphere (known) and the solar irradiance reflected back to space (derived from GOCI radiance), taking into account absorption and scattering by the clear atmosphere (modeled). Knowledge of pixel composition is not required. Apart from planetary albedo and sun zenith angle, the model parameters are fixed at their climatological values. The instantaneous PAR estimates at hourly intervals are integrated over time to provide daily values. The technique is applied to GOCI imagery acquired on 5 April 2011, and the GOCI daily PAR estimates are compared with those obtained from MODerate Resolution Imaging Spectrometer (MODIS) data. Agreement is good between the two types of estimates, with a coefficient of determination (r^2) of 0.778, a bias of 0.23 $Em^{-2}d^{-1}$ (0.5% with higher GOCI values), and a root-mean-squared difference of 5.00 $Em^{-2}d^{-1}$ (11.2%). Differences in cloudy conditions are attributed to daily cloudiness changes not captured by the MODIS observations. The comparison statistics indicate that GOCI PAR estimates have acceptable accuracy for regional studies of aquatic photosynthesis.

Key words – light, photosynthesis, phytoplankton, marine ecosystems

1. Introduction

The solar energy available for aquatic photosynthesis, known as PAR, controls the growth of phytoplankton and, therefore, regulates the composition and evolution of marine ecosystems (Kirk 1996). Sunlight in the ocean also warms the surface layers and, therefore, modifies the density contrast between the mixed layer and deeper layers. The resulting variations in the depth and temperature of the mixed layer play a major role in the physical climate. Knowing the spatial and temporal distribution of PAR over the East-Asia Seas is critical to understanding biogeochemical cycles of carbon, nutrients, and oxygen in the region, and to address important climate issues such as the fate of anthropogenic atmospheric carbon dioxide.

The PAR data sets expected to be available during the operational phase of GOCI are essentially those produced from SeaWiFS and MODIS data by NASA's Ocean Biology Processing Group (OBPG) using the algorithm developed by Frouin et al. (2003). Accuracy of the products on a daily time scale is chiefly limited by the lack of information about diurnal variability of clouds, since the instruments are onboard sun-synchronous platforms. Total solar irradiance data sets routinely produced from GMS VISSR hourly observations (Kawai and Kawamura 2005) could be used, but conversion to PAR is subject to uncertainties (e.g., Frouin and Pinker 1995; Frouin and Murakami, 2007). Furthermore, the spatial resolution of the SeaWiFS, MODIS, and VISSR data sets is 9 km, 4 km, and 0.5 degree, respectively, i.e., it does not match the higher resolution (0.5 km) of the GOCI ocean-color observations.

In view of the importance of PAR for GOCI science applications and the limitations of available PAR data sets, a technique has been developed to estimate PAR from GOCI data. The sensor is adapted to the problem, since it measures in the PAR spectral range and has a large dynamic

*Corresponding author. E-mail: rfrouin@ucsd.edu

range (i.e., it does not saturate over clouds). Importantly, observations are made every hour, which provides adequate temporal sampling to handle the diurnal variability of clouds. Furthermore, it is most convenient, for primary productivity computations, to derive both PAR and chlorophyll abundance from the same ocean-color sensor.

The technique is based on previous work reported in Frouin and Chertock (1992), Frouin et al. (2003), and Frouin and Murakami (2007). Instantaneous PAR at the GOCI observation times is computed as the difference between the incident solar flux at the top of the atmosphere (known) and the solar irradiance reflected back to space (derived from GOCI radiance), taking into account atmospheric absorption and scattering by the clear atmosphere. Apart from planetary albedo and sun zenith angle (the most important parameters governing surface solar irradiance variability), the model input parameters, namely ozone and water vapor amounts, aerosol optical thickness and Angström exponent, and surface albedo, are fixed at their climatological values. For each GOCI pixel, the instantaneous PAR estimates are integrated over time, sunrise to sunset, to provide daily PAR values.

In the present article, the technique developed to estimate surface PAR from GOCI data is described. Simplifying assumptions are discussed, as well as advantages and limitations, especially the technique's ability to capture the diurnal variability of clouds. The technique is applied to GOCI imagery acquired on April 5, 2011 and the PAR daily estimates are compared with those from MODIS data, which have been evaluated against in situ measurements. Comparisons are also made between daily PAR estimates obtained from a single and from all (i.e., eight) GOCI observations, the single observation case corresponding to instruments in sun-synchronous orbit. In view of performance and the uncertainty on physiological parameters influencing primary productivity, conclusions are made on the technique's adequacy to meet accuracy requirements for biogeochemistry applications.

2. Methodology

The technique estimates daily (i.e., 24-hour averaged) PAR reaching the ocean surface. Since photosystem processes are quantum reactions, PAR is defined as the quantum energy flux from the Sun in the spectral range 400-700 nm. It is expressed in units of Einstein per meter squared per day, i.e., $Em^{-2}day^{-1}$.

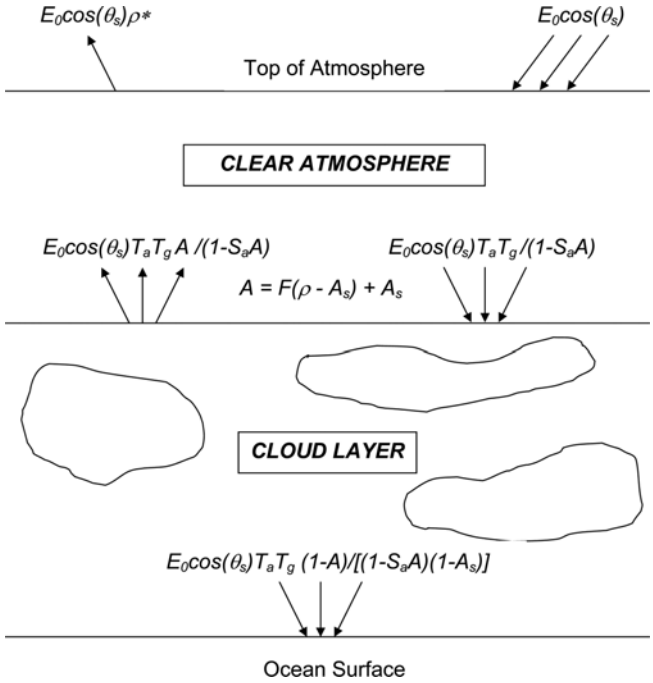

Fig. 1. Schematic diagram of the PAR model. The clear atmosphere is located above a cloud layer. For each GOCI observation (i.e., each θ_s) and spectral band in the PAR range, the albedo of the cloud/surface layer system, A, is obtained from the GOCI reflectance ρ^* corrected for gaseous absorption and scattering by the clear atmosphere, ρ. The flux reaching the surface is computed as the difference between the reflected flux and the incoming flux at the top of the cloud/surface layer, taking into account the surface albedo A_s (See text for details.)

The PAR model uses plane-parallel theory and assumes that the effects of clouds and other atmospheric constituents can be de-coupled. The planetary atmosphere is therefore modeled as a clear-sky atmosphere positioned above a cloud/surface layer, and surface PAR is expressed as the product of a clear-sky component and cloud transmittance (see Fig. 1). This approach was shown to be valid by Dedieu et al. (1987) and Frouin and Chertock (1992). The great strength of such a de-coupled model resides in its simplicity. It is unnecessary to distinguish between clear and cloudy regions within a pixel, and this dismisses the need for often-arbitrary assumptions about cloudiness distribution.

Under solar incidence θ_s, the incoming solar flux at the top of the atmosphere, $E_0\cos(\theta_s)$, is reduced by a factor $T_aT_g/(1-S_aA)$ by the time it enters the cloud/surface system. In this expression, T_a is the clear-sky diffuse transmittance (due to scattering by molecules and aerosols), T_g is the gaseous transmittance (essentially due to absorption by ozone), S_a is

the spherical albedo, and A is the cloud/surface system albedo. As the flux, $E_0\cos(\theta_s)T_aT_g/(1-S_aA)$, passes through the cloud/surface system, it is further reduced by a factor A. The solar flux reaching the ocean surface, E, is then given by

$$E=E_{clear}(1-A)(1-A_s)^{-1}(1-S_aA)^{-1}, \quad (1)$$

where A_s is the albedo of the ocean (surface and water body) and $E_{clear}=E_0\cos(\theta_s)T_d\,T_g$ is the solar flux that would reach the surface if the cloud/surface system were non reflecting and non-absorbing. In clear sky conditions, A reduces to A_s and E to $E_{clear}(1-S_aA_s)^{-1}$. Under the plane-parallel assumption, A can be written as:

$$A=NA'_c+(1-N)A_s, \quad (2)$$

where N is the cloud fraction and A'_c is the cloud contribution to A, including multiple surface reflections. For a non-absorbing cloud of albedo A_c,

$$A'_c=A_c+(1-A_c)^2A_s/(1-A_cA_s). \quad (3)$$

Using (2), the expression for A becomes:

$$A\approx NA_c+A_s, \quad (4)$$

where the denominator in (3) is approximated by $(1+A_cA_s)$ and the term in A_cA_s and higher-order terms in A_c and A_s have been neglected. Note that clouds do not absorb in the PAR spectral range.

In order to compute E, A is expressed as a function of the radiance measured by GOCI in the PAR spectral range, i.e., in bands centered at 412, 443, 490, 555, and 660 and 680 nm (bands 1 through 6, respectively). The algorithm works pixel by pixel and proceeds as follows.

First, for each pixel not contaminated by sun glitter, which is generally the case with GOCI, the GOCI bidirectional radiance L_i* in band i, expressed in $\mathrm{mWcm^{-2}\mu m^{-1}sr^{-1}}$, is transformed into reflectance, ρ_i*:

$$\rho_i^*=\pi L_i^*/[E_{0i}\cos(\theta_s)], \quad (5)$$

where E_{0i} is the extra-terrestrial solar irradiance in band i, and θ_s is the sun zenith angle at the GOCI observation time. Note that E_{0i} in (5) takes into account the actual Earth-Sun distance. Sun glint areas are excluded because they would be interpreted as cloudy in the PAR algorithm.

Second, the GOCI reflectance ρ_i* is corrected for ozone absorption:

$$\rho_i'=\rho_i^*/T_{gi} \quad (6)$$

with

$$T_{gi}=\exp[-k_{oi}U_o(1/\cos(\theta_s)+1/\cos(\theta_v)], \quad (7)$$

where k_{oi} is the ozone absorption coefficient in band i, U_o is the ozone amount, and θ_v is the viewing zenith angle. The k_{oi} values are obtained from the 6S code (Vermote et al. 1997), and the U_o values are taken from satellite-derived climatology.

Third, the reflectance of the cloud/surface layer, ρ_i, is obtained from ρ_i' following Tanré et al. (1979) and assuming isotropy of the cloud/surface layer. We have

$$\rho_i=(\rho_i'-\rho_{ai})[T_{ai}(\theta_{sj})T_{ai}(\theta_v)+S_{ai}(\rho_i'-\rho_{ai})]^{-1}, \quad (8)$$

where ρ_{ai} is the intrinsic atmospheric reflectance in band i (represents photons that have not interacted with the cloud/surface layer). The assumption of isotropy is crude, but is made because no information on pixel composition is available.

In (8), ρ_a is modeled using the quasi single-scattering approximation:

$$\rho_a=(\tau_{mol}P_{mol}+\omega_{aer}\tau_{aer}P_{aer})[4\cos(\theta_s)\cos(\theta_v)]^{-1}, \quad (9)$$

where τ_{mol} and τ_{aer} are the optical thicknesses of molecules and aerosols, P_{mol} and P_{aer} are their respective phase functions, and ω_{aer} is the single scattering albedo of aerosols. In (9), the optical parameters depend on wavelength, but subscript i has been omitted for clarity. The quasi single-scattering approximation is inaccurate at large zenith angles, but at those angles the solar flux is small. The diffuse transmittance T_a and spherical albedo S_a are computed using analytical formulas developed by Tanré et al. (1979):

$$T_a(\theta)=\exp[-(\tau_{mol}+\tau_{aer})/\cos(\theta)]\exp[(0.52\,\tau_{mol}+0.83\,\tau_{aer})/\cos(\theta)] \quad (10)$$

$$S_a=(0.92\,\tau_{mol}+0.33\,\tau_{aer})\exp[-(\tau_{mol}+\tau_{aer})], \quad (11)$$

where τ_{mol} is the optical thickness of molecules, τ_{aer} that of aerosols, and θ is either θ_s or θ_v.

The optical thickness of aerosols in band i, τ_{aeri}, is obtained from the optical thickness at the reference wavelength λ_0, τ_{aer0}, and the Angström coefficient between λ_i and λ_0, α:

$$\tau_{aeri}=\tau_{aer0}(\lambda_0/\lambda_i)^a, \quad (12)$$

where λ_0 is equal to 865 nm (GOCI band 8). A monthly climatology based on several years of MODIS data is used for τ_{aer0} and α, since aerosol properties cannot be determined when the pixel is cloudy. This procedure is also justified because, in general, aerosol effects on E are secondary compared with cloud and θ_s effects.

To estimate ω_{aer} and P_{aer}, the two closest aerosol models, k and l, in a set of models (the models used in the standard atmospheric correction of SeaWiFS and MODIS) that verify $\alpha(l)<\alpha<\alpha(k)$ are selected, and a distance $d_{aer}=[\alpha(l)-\alpha]/[\alpha(l)-\alpha(k)]$ is computed. Using this distance, ω_{aer} and P_{aer} are obtained as follows:

$$\omega_{aer}=d_{aer}\omega_{aer}(k)+(1-d_{aer})\omega_{aer}(l) \quad (13)$$

$$P_{aer}=d_{aer}P_{aer}(k)+(1-d_{aer})P_{aer}(l), \quad (14)$$

where $\omega_{aer}(l)$ and $\omega_{aer}(k)$ are the single scattering albedos of aerosol models l and k, and $P_{aer}(l)$ and $P_{aer}(k)$ their respective phase functions.

Once the reflectance of the cloud/surface layer, ρ, is determined, it is converted into albedo A. This is accomplished for all the spectral bands by applying a cloud bidirectional correction factor F (independent of wavelength) to $\rho-A_s$, see (4):

$$A = F(\rho - A_s) + A_s. \quad (15)$$

Instead of statistical angular models (e.g., Young et al. 1998), analytical formulas developed by Zege (1991) for non-absorbing and optically thick scattering layers are used. In (15), the surface albedo A_s is parameterized as a function of sun zenith angle and aerosol optical thickness at 500 nm, following Jin et al. (2004). This parameterization takes into account Fresnel reflection and under-light scattering, but does not explicitly include wind speed and chlorophyll concentration effects. If $\rho > A_s$, which indicates the presence of clouds, a formula for completely diffuse sky is used.

The various functions or parameters in (1), namely A, A_s, T_g, T_d, and S_a, are computed for each GOCI spectral band in the visible spectrum and for each GOCI hourly observation. In the next step, they are transformed into average values over the PAR spectral range by integrating over wavelength the spectral values weighted by the corresponding extraterrestrial solar irradiance and normalizing by the total (i.e., 400 to 700 nm) extraterrestrial irradiance.

Finally, daily PAR is computed by integrating (1) over the length of the day by the simple trapezoidal rule:

$$PAR = (1/24)\ E_{0PAR}\ \Sigma_j\ (G_{j+1} + G_j)(t_{j+1}-t_j)/2 \quad (16)$$

with

$$G_j=\cos(\theta_{sj})<T_{gj}><T_{aj}>(1-<A_j>)/[(1-<A_{sj}>)(1-<S_a><A_j>)] \quad (17)$$

where E_{0PAR} is the extraterrestrial solar irradiance over the PAR range, index j denotes the GOCI observation time t_j, and <> is average value over the PAR range. We have $j = 0$ to 9, with $j = 0$ corresponding to sunrise ($G_0 = 0$), $j = 9$ to sunset ($G_9 = 0$), and $j = 1$ to 8 to the eight GOCI observations during the day. Note that S_a does not depend on geometry. The other parameters depend on θ_{sj}, the sun zenith angle at the time of observation.

3. Application to GOCI Data

The methodology has been applied to GOCI imagery acquired on April 5, 2011 at 00:16, 01:16, 02:16, 0.3:16, 04:16, 05:16, 06:16, and 07:16 GMT. Fig. 2 displays a RGB composite of the 03:16 GMT image. The East Sea and the Yellow Sea are practically free of clouds, but a large cloud system is present southeast of Japan. In all spectral bands, the top-of-atmosphere radiance is relatively low and narrowly distributed over the clear-sky areas, but exhibits higher values and large spatial variability over the cloudy region (Fig. 3). At 680 nm (Band 6), for example, the values are concentrated around 20 $Wm^{-2}sr^{-1}\mu m^{-1}$ above clear skies, but they vary between 30 and 100 $Wm^{-2}sr^{-1}\mu m^{-1}$ above cloudy skies, the highest values being encountered over

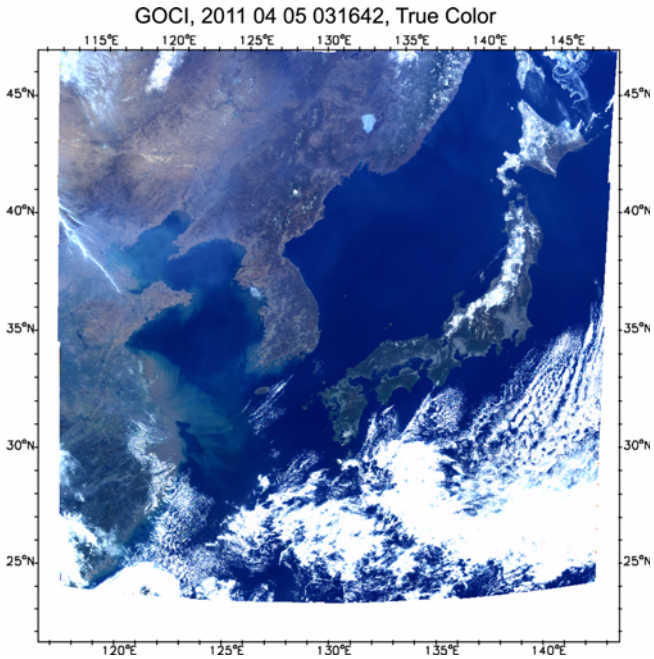

Fig. 2. GOCI true color image acquired on April 5, 2011 at 03:16 GMT showing clear atmosphere over the East Sea and the Yellow Sea and clouds South and Southeast of Japan

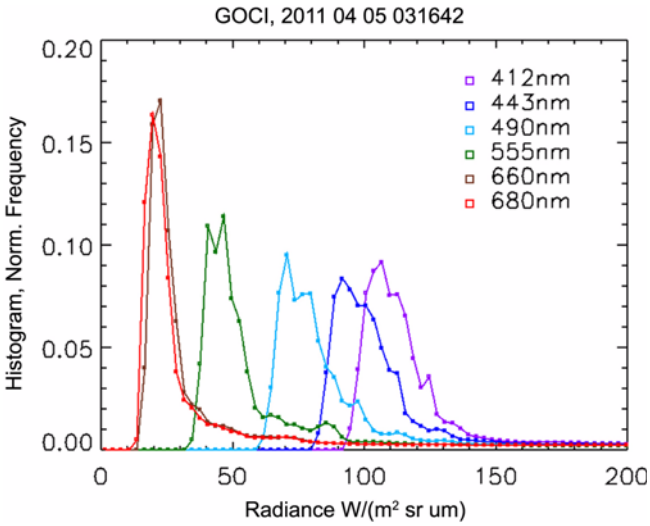

Fig. 3. Histograms of top-of-atmosphere radiance in the first 6 GOCI spectral bands for GOCI imagery of April 5, 2011 at 03:16 GMT

convective clouds. The histograms of Fig. 3 do not reveal any saturation over reflective clouds.

During the course of the day, the top-of-atmosphere radiance varies quite differently with the absence or presence of clouds (Fig. 4). In the absence of clouds (sub-area centered on 40°N and 134°E), the diurnal variability is smooth, following changes in the cosine of the sun zenith angle. In the presence of clouds (sub-area centered on 28°N and 136°E), the diurnal variability is more erratic, with large standard deviation, reflecting changes in cloudiness (e.g., displacement, generation, and disappearance). This suggests that multiple observations during the day are needed to describe adequately cloud variability.

The daily PAR results obtained using all the GOCI hourly observations are displayed in Fig. 5 (top). Values are high in the clear-sky areas (and higher as the latitude decreases due to smaller sun zenith angle), reaching about 55 $Em^{-2}d^{-1}$ in the East China Sea, and lower in the cloudy areas, with values as small as 12 $Em^{-2}d^{-1}$. In the Bohai Sea and the West part of the Yellow Sea (Yangtze effluent), PAR exhibits slightly lower values compared with the clear sky values at similar latitudes. This is due to a higher surface albedo than the one used in the modeling (based on Lin et al. 2004), i.e., the algorithm interprets the data as being contaminated by thin clouds. The situation can be remedied, however, by using for surface reflectance, and therefore albedo, the lowest reflectance imagery at each observation time during a certain interval (e.g., a week).

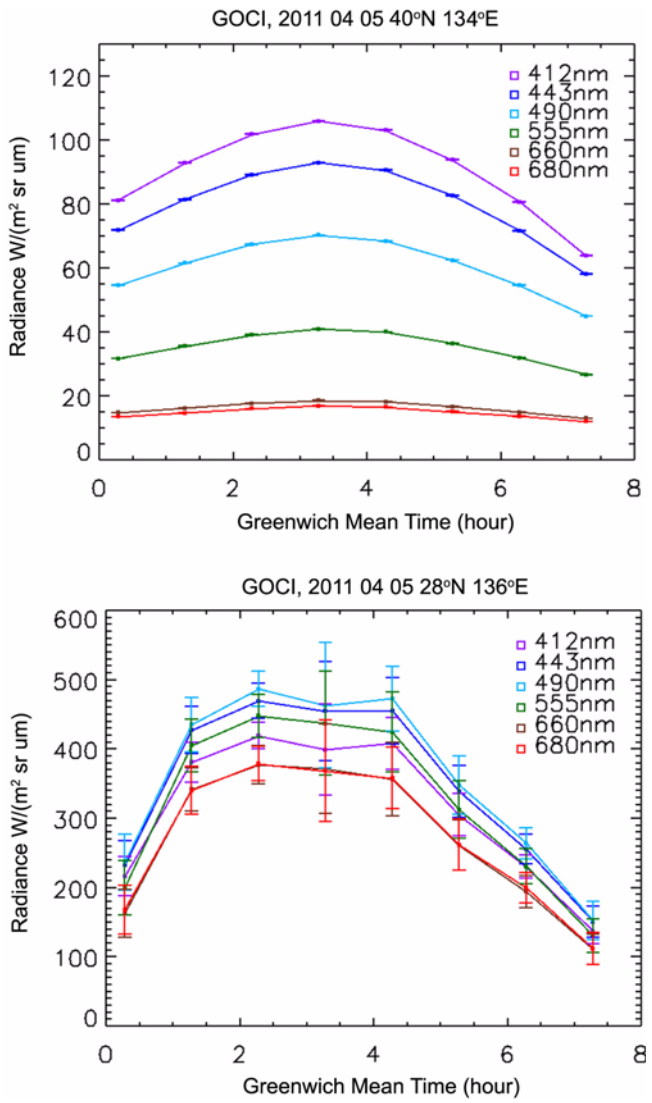

Fig. 4. Evolution of the top-of-atmosphere GOCI radiance during April 5, 2011 in a clear-sky area centered on 40°N and 134°E (top) and a cloudy area centered on 28°N and 136°E (bottom). The size of the areas is 10×10 pixels

Since instruments on polar orbiters (SeaWiFS, MODIS) observe typically once a day, except at high latitudes, the PAR estimated using the eight hourly observations have been compared with those estimated using a single hourly observation. Fig. 5 (bottom) displays the PAR imagery obtained with only GOCI data acquired at 3:16 GMT. In clear-sky regions, the PAR values are similar to those obtained with all of the observations, which is expected since in this case the governing parameter is essentially the Sun zenith angle (satellite observations have little or no impact on estimating clear-sky PAR). In cloudy regions, the PAR

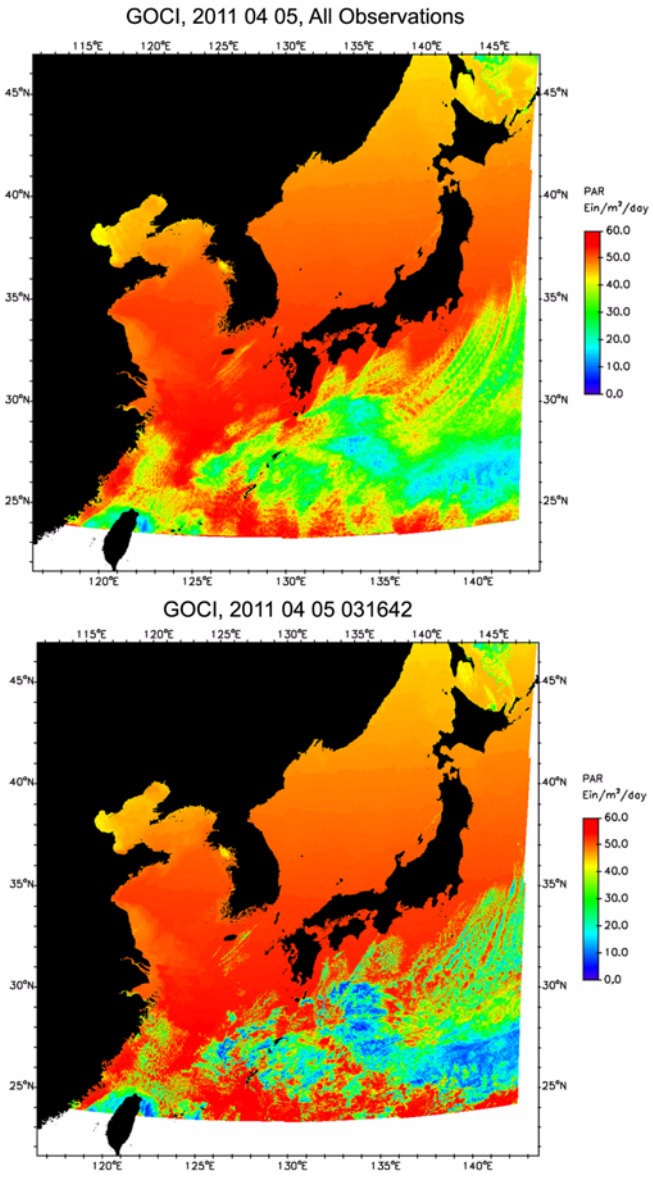

Fig. 5. Daily PAR imagery for April 5, 2011 obtained from eight GOCI observations at 00:16, 01:16, 02:16, 0.3:16, 04:16, 05:16, 06:16, and 07:16 GMT (top) and a single GOCI observation at 03:16 GMT (bottom)

values exhibit less spatial variability (i.e., the spatial field is smoother) due to changes in cloudiness accounted for in the daily average. This is also observed in Fig. 6, which depicts histograms of PAR values estimated using eight observations per day (blue curve) and a single observation per day (red curve). The range of PAR values is larger with one observation per day, especially at the low end, with values extending to 5 $Em^{-2}d^{-1}$ (instead of 12 $Em^{-2}d^{-1}$), and there are many less values between 20 and 45 $Em^{-2}d^{-1}$. In terms of comparison statistics, the two types of estimates exhibit a coefficient of

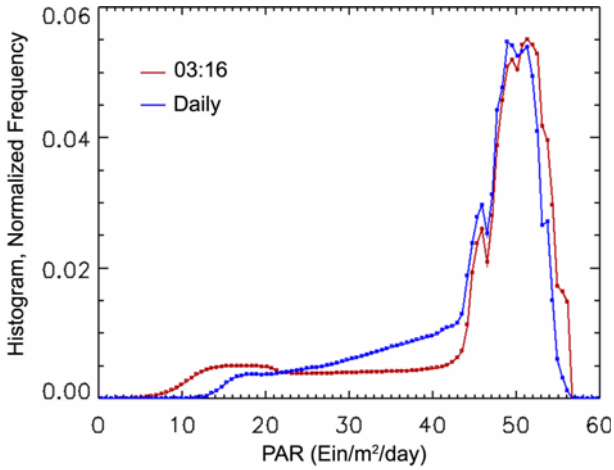

Fig. 6. Histogram of daily PAR values obtained using GOCI observation at 03:16 GMT and all observations during April 5, 2011 (red and blue curves, respectively)

determination (r^2) of 0.758, a bias of 0.11 $Em^{-2}d^{-1}$ (0.2%), i.e., slightly higher values using a single observation, and a root-mean-squared (RMS) difference of 5.92 $Em^{-2}d^{-1}$ (13.5%), largely due to cloudy situations.

4. Evaluation using MODIS Data

Since no in situ PAR measurements were available in the study region, the GOCI PAR estimates have been compared with MODIS-Terra and MODIS-Aqua estimates produced by NASA's OBPG. These estimates have been evaluated against PAR data collected during 2005-2010 at the CERES Ocean Validation Experiment (COVE) site off Chesapeake Bay in the North Atlantic (latitude similar to the latitude of Seoul). Compared with in situ measurements, the MODIS estimates (Aqua and Terra, respectively) are higher by 1.8 and 2.3 $Em^{-2}d^{-1}$ (4.5 and 5.7%) on a daily time scale, and they exhibit r^2 values of 0.857 and 0.883 and RMS errors of 6.8 and 6.3 $Em^{-2}d^{-1}$ (about 16%). The biases are due to uncertainties in the clear sky model (e.g., calculation of spectrally integrated transmittance functions) and the diurnal variability of cloudiness not fully accounted for in the algorithm. At the COVE site, a maritime non-convective location, cloud cover tends to be higher in the morning and afternoon, and the times of satellite overpass are generally in the middle of the day.

The comparisons have been made at the MODIS Level 3 resolution, i.e., 4×4 km, and the GOCI estimates at 0.5 km resolution have therefore been remapped to that grid. A

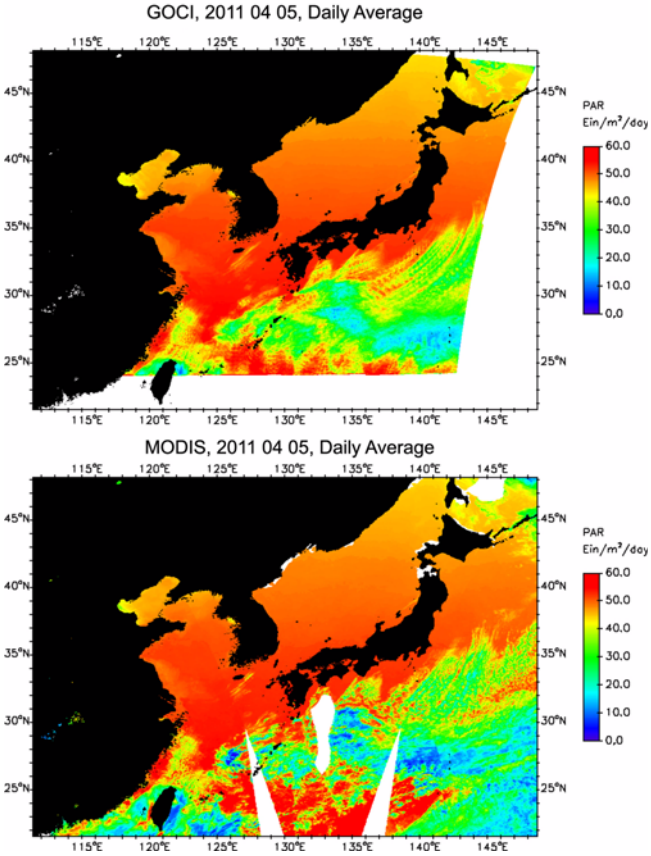

Fig. 7. Daily PAR imagery for April 5, 2011 obtained from GOCI data (top) and MODIS-Aqua and -Terra data (bottom). The GOCI estimates at 0.5 km resolution are remapped onto the MODIS Level 3 4×4 km grid

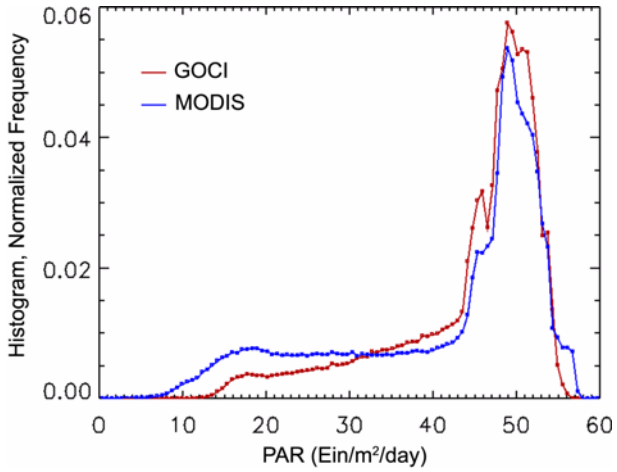

Fig. 8. Histograms of daily PAR values (April 5, 2011) obtained at L3 resolution using GOCI data (red curve) and MODIS-Aqua and -Terra data (blue curve)

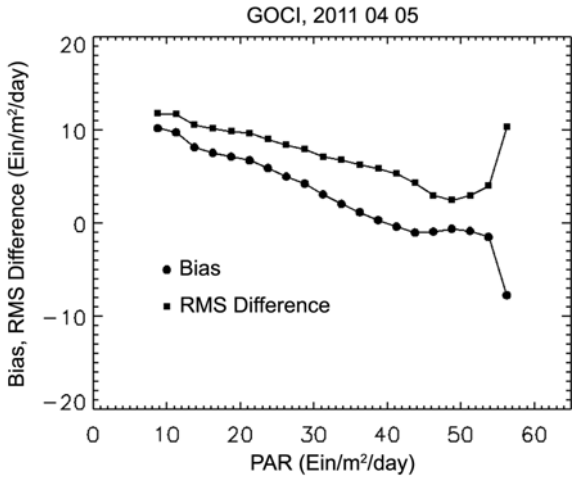

Fig. 9. Bias and RMS difference between GOCI and MODIS daily PAR values versus PAR level for April 5, 2011

composite of The MODIS-Aqua and MODIS-Terra products was created by simple average. Note that the GOCI and MODIS clear sky model had been compared, since they do not use the same spectral bands, and the GOCI values were adjusted accordingly. This adjustment, i.e., a reduction of about 5%, had also been made in Fig. 5.

Fig. 7 displays the GOCI PAR imagery and corresponding MODIS imagery on the Level 3 grid (top and bottom, respectively). The missing PAR data in the MODIS imagery correspond to sun glint conditions (PAR is not computed in such situations) or missing MODIS data. Like in Fig. 5 (top) compared with Fig. 5 (bottom), the MODIS PAR values in cloudy regions, obtained with one or two observations during the day, exhibit a larger range of variability than the GOCI values, with differences between the two types of estimates mostly between -10 and 10%. The histograms of PAR values also indicate that, in the presence of clouds, the GOCI PAR estimates cover a lower range of values (Fig. 8).

In clear-sky conditions, the differences are generally below 1% in magnitude. The comparison statistics, i.e., r^2 of 0.778, bias of 0.22 $Em^{-2}d^{-1}$ (0.5%), and RMS difference of 5.00 $Em^{-2}d^{-1}$ (11.2%) indicate agreement between the two types of estimates. The good performance, however, much better than the MODIS performance against in situ measurements (see above), should be interpreted in view of the fact that a large part of the April 5, 2011 GOCI imagery is free of clouds, i.e., a situation for which the GOCI and MODIS PAR values are expected to be close. In cloudy conditions, the performance is degraded, as evidenced in Fig. 9, which displays bias and RMS difference as a function of PAR level. At low PAR values, for example, the bias and RMS difference are about 10 and 12 $Em^{-2}d^{-1}$ at 6.5

$Em^{-2}d^{-1}$, respectively, i.e., substantially larger than for the entire image (i.e., both clear and cloudy pixels). Above PAR values of 50 $Em^{-2}d^{-1}$, the RMS difference increases with PAR level and the bias becomes more negative (lower GOCI values). This is explained by MODIS observing clear sky conditions in the lower part of the image and GOCI capturing cloudiness changes during the day.

5. Conclusions

A technique originally developed to estimate daily PAR at the ocean surface from SeaWiFS and MODIS data has been adapted to GOCI data. The chief advantage of using GOCI data is the ability to describe properly the diurnal variability of clouds. The solar irradiance modeling is simplified, with PAR expressed as the product of a clear-sky component and a cloud transmittance, but the essential physics is included. The albedo of the cloud/surface system is determined from the GOCI radiance, which requires transforming the top-of-atmosphere bidirectional signal into albedo, after correcting for scattering and absorption by the clear atmosphere. The crude treatment of clouds in the modeling, including their bidirectional properties, makes the technique inherently less accurate in cloudy conditions. Large errors in the instantaneous PAR values are expected in some situations, for example broken clouds and cloud shadows, but these errors are generally reduced in daily averages. Also the surface albedo parameterization, based on measurements at an open-ocean site, may not be suitable for coastal turbid waters, since the higher actual albedo may be interpreted as a thin cloud, reducing the PAR estimate.

The technique has been applied to GOCI data acquired on April 5, 2011, and the resulting PAR estimates have been compared with MODIS estimates provided by NASA and evaluated against in situ measurements. The two types of estimates are in agreement, with little bias (<1%) and a RMS difference of 11.2%. Estimating daily PAR using eight observations per day instead of one observation per day, which is the case of instruments on sun-synchronous satellites, tends to reduce the range of PAR values and introduce cloudiness-dependent differences that may not be systematic or region-characteristic. Importantly, the comparative analysis has been made using one day of GOCI data, which is obviously insufficient to draw definite conclusions about accuracy. Additional imagery needs to be examined, during various atmospheric conditions and seasons, and the GOCI estimates should be evaluated directly against in situ measurements (e.g., by establishing a dedicated program with PAR instruments installed on offshore platforms).

In view of the accuracy of the MODIS estimates, the results obtained with GOCI data indicate good algorithm performance for studies of aquatic photosynthesis. Note in this respect, that primary productivity models depend, not only on PAR, but also on efficiency factors that are difficult to estimate with accuracy comparable to that of PAR. It is expected that a long-term PAR data set will be generated using the proposed technique during the GOCI operational phase. The data set will be unique and invaluable, allowing a wide range of research applications, such as primary production and carbon export modeling, ecosystem development and mixed-layer physics, and photochemical transformations of dissolved organic matter. This will contribute significantly to understanding the role of the Northwestern Pacific Ocean and East-Asia Seas in carbon cycling and climate change.

Note finally that the methodology can be easily extended to compute ultraviolet (UV), i.e., UV-A and UV-B, irradiance. Cloud properties (extinction coefficient, asymmetry factor) are similar in the UV and PAR spectral range, i.e., the effects of clouds on UV irradiance may be estimated from effects in the PAR spectral range. The scientific applications are numerous, since enhanced UV irradiance may inhibit phytoplankton photosynthesis, increase ocean transparency (photo-oxidation of CDOM), increase bioavailability of nutrients, etc. Furthermore, surface reflectance can be estimated over both land and ocean from a time series of GOCI images (e.g. minimum value over a week), allowing more accurate PAR estimates in coastal turbid regions and providing PAR estimates over land.

Acknowledgements

This work was supported by the National and Aeronautics Administration (NASA) under Grants NNX08AL78A and NNX11AQ22G, and by the Korean Ocean Research and Development Institute. The NASA Ocean Biology Processing Group, which operationally generates SeaWiFS and MODIS PAR products, is gratefully acknowledged.

References

Dedieu G, Deschamps P-Y, Kerr YH (1987) Satellite estimation of

solar irradiance at the surface of the earth and of surface albedo using a physical model applied to Meteosat data. J Clim Appl Meteorol **26**:79-87

Frouin R, Chertock B (1992) A technique for global monitoring of net solar irradiance at the ocean surface. Part I: Model. J Appl Meteorol **31**:1056-1066

Frouin R, Pinker RT (1995) Estimating photosynthetically active radiation (PAR) at the Earth's surface from satellite observations. Remote Sens Environ **51**:98-107

Frouin R, Franz BA, Werdell PJ (2003) The SeaWiFS PAR product. In: Algorithm Updates for the Fourth SeaWiFS Data Reprocessing. NASA/TM-2003-206892, pp 46-50

Frouin R, Murakami H (2007) Estimating photosynthetically available radiation at the ocean surface from ADEOS-II Global Imager data. J Oceanogr **63**:493-503

Jin Z, Charlock TP, Smith WL, Rutledge K (2004) A parameterization of ocean surface albedo. Geophys Res Lett **31**. doi:10.1029/2004GL021180

Kawai Y, Kawamura H (2005) Validation and improvement of satellite-derived surface solar radiation over the Northwestern Pacific Ocean. J Oceanogr **61**:79-89

Kirk JTO (1996) Light and Photosynthesis in Aquatic Ecosystems, 3nd edition. Cambridge University Press, 509 p

Tanré D, Herman M, Deschamps P-Y, De Leffe A (1979) Atmospheric modeling for space measurements of ground reflectances, including bi-directional properties. Appl Opt **18**:3587-3594

Vermote E, Tanré D, Deuzé J-L, Herman M, Morcrette J-J (1997) Second simulation of the satellite signal in the solar spectrum: an overview. IEEE Trans Geosci Remote Sens **35**:675-686

Young DF, Minnis P, Doelling DR, Gibson GG, Wong T (1998) Temporal interpolation methods for the Clouds and Earth's radiant Energy System (CERES) experiment. J Appl Meteorol **37**:572-590

Zege EP, Ivanov AP, Katsev IL (1991) Image Transfer through a Scattering Medium. Springer-Verlag, New York, 349 p